

Energy Storage Optimization for Grid Reliability

Md Umar Hashmi, Ana Bušić
INRIA, Ecole Normale Supérieure,
CNRS, PSL Research University,
Paris, France
md-umar.hashmi,ana.busic@inria.fr

Deepjyoti Deka
Theoretical Division,
Los Alamos National Laboratory
New Mexico, USA
deepjyoti@lanl.gov

Lucas Pereira
ITI, LARSyS, Técnico Lisboa,
and prsma.com,
Funchal, Portugal
lucas.pereira@iti.larsys.pt

ABSTRACT

Large scale renewable energy source (RES) integration planned for multiple power grids around the world will require additional resources/reserves to achieve secure and stable grid operations to mitigate the inherent intermittency of RES. In this paper, we present formulations to understand the effect of fast storage reserves in improving grid reliability under different cost functions. Our formulations not only aim to minimize imbalance but also maintain state-of-charge (SoC) of storage. The proposed approaches rely on a macroscopic supply-demand model of the grid with total power output of energy storage as the control variable. We show that accounting for system response due to inertia and local governor response enables a more realistic quantification of storage requirements for damping net load fluctuations. Simulation case studies are embedded in the paper by using datasets from the Elia TSO in Belgium and BPA in the USA. The numerical results benchmark the marginal effect on reliability due to increasing storage size under different system responses and associated cost functions. Further we observe myopic control of batteries proposed approximates deterministic control of batteries for faster time scale reserve operation.

CCS CONCEPTS

• **Software and its engineering** → *Power management*; Real-time systems software.

KEYWORDS

Storage optimization, grid reliability, SAIDI, frequency response, McCormick relaxation, real-time operation, myopic algorithm.

ACM Reference Format:

Md Umar Hashmi, Ana Bušić, Deepjyoti Deka, and Lucas Pereira. 2020. Energy Storage Optimization for Grid Reliability. In *The Eleventh ACM International Conference on Future Energy Systems (e-Energy'20)*, June 22–26, 2020, Virtual Event, Australia. ACM, New York, NY, USA, 7 pages. <https://doi.org/10.1145/3396851.3402123>

Permission to make digital or hard copies of all or part of this work for personal or classroom use is granted without fee provided that copies are not made or distributed for profit or commercial advantage and that copies bear this notice and the full citation on the first page. Copyrights for components of this work owned by others than ACM must be honored. Abstracting with credit is permitted. To copy otherwise, or republish, to post on servers or to redistribute to lists, requires prior specific permission and/or a fee. Request permissions from permissions@acm.org.
e-Energy'20, June 22–26, 2020, Virtual Event, Australia
© 2020 Association for Computing Machinery.
ACM ISBN 978-1-4503-8009-6/20/06.
<https://doi.org/10.1145/3396851.3402123>

1 INTRODUCTION

Massive installation of solar and wind resources in power grids is slated to replace conventional sources of power. As renewable generation is a function of weather parameters such as solar irradiance and wind speed, such sources are inherently uncertain/stochastic. For instance, solar generation could fluctuate more than 70% due to passing clouds during daytime and wind generation could ramp down 100% due to loss of wind [9]. As the share of renewable generation has increased, the amount curtailment has also proportionally increased, with a total cumulative curtailed energy of 1817 GWh from May 2014 to April 2019 in CAISO [4].

Traditional resources, due to the presence of rotation mass, provide system inertia to counter fluctuations [22]. The absence of inertia in several inverter corrected renewable resources compounds the problem of managing variability, when penetration levels increase further [11]. To ensure power system reliability, utilities have to hold ramp-up and ramp-down reserves in order to compensate for sudden loss of renewable generation. The authors in [18] observe that, to accommodate 15% of wind generation, traditional reserves have to be increased upto 9%. In order to compensate the renewable volatility and avoid massive reserve procurement, additional fast ramping resources, with associated performance based payments [31] are being incorporated. The authors in [17] observe that energy storage systems can mitigate issues with large scale renewable integration due to their fast ramping. Falling cost of Li-Ion batteries (and other energy storage technologies) has encouraged the bulk installation of batteries for this purpose [3]. While it is true that increasing energy storage can in theory lead to improvement in reliability, their true performance depends on available conventional responsive resources. Following a net imbalance in injection, the complete system response, due to conventional generation and fast ramping batteries, determines the dynamics in operational frequency, including the maximum deviation in frequency (termed 'nadir') and the time to reach there [22]. This is utilized by grid operators to determine reserves necessary to ensure secure operations [8]. The overarching goal of this work is to *quantify* the effect of storage, including its marginal value, on reliability by accounting for the system response in the presence of system inertia and generator governors.

1.1 Prior Work

Optimization of storage operations is a growing field of research. Storage usage for arbitrage and peak shaving operates at a slower time scale (minutes-hours to weeks) and has been analyzed in [6, 14, 16, 23, 26, 28]. In work associated with storage usage for reliability, the authors in [5] consider investor-owned reserves that perform bidding to profitably provide balancing services [15]. In [27], storage along with energy dissipating resistors are used for

primary frequency control. The authors of [21] use energy storage for providing inertial response along with primary frequency regulation and show that response similar to conventional power plants can be derived. [30] looks at the impact of energy storage parameters such as capacity, ramping parameters and conversion efficiency on the impact of renewable integration. [7] observes that myopic control algorithms for storage operation can approximate deterministic solution for cases with small time-difference between decisions. [29] looks at the utility's problem of minimizing power imbalance by using storage devices and presents threshold based control rules, however they ignore system response in their analysis. [10] shows that reserve sizing based on worst-case imbalance would not be financially plausible. Bringing the reliability requirement and system response into the picture can help in understanding the marginal increase in reliability due to integrating energy storage as reserves.

1.2 Contributions of the paper

We consider centralized optimization of utility owned/operated storage for improving grid reliability. While the profitability of battery is crucial, we assume payment for capacity to owners and do not include electricity prices while optimizing storage actions in real-time [31]. Rather, we are interested in identifying marginal system-wide reliability improvement due to available storage. We first justify a relaxed system reliability index measured in terms of net power balance that is principally aware of the conventional bulk system response due to inverters and governors. For both linear and quadratic cost functions of net imbalance, we present convex but non-smooth optimization formulations for real-time storage operation. The storage optimization problem can also incorporate state of charge (SoC) based constraints to ensure ramping availability during unexpected large imbalances. We present McCormick relaxation and threshold based exact schemes for our formulations, and benchmark the performance with respect to different reliability metrics, using real imbalance information from two regions: (a) Elia TSO in Belgium and (b) BPA (Bonneville Power Administration) in USA. Our work demonstrates that while increase in storage improves reliability, the *marginal value of integrating storage deteriorates with the storage size*. More importantly, *the computed decrease in marginal benefit is more severe for systems with higher system response*. As our optimal solutions are deterministic and require information of all fluctuations, we compare them with a myopic storage algorithm that uses only current information. We observe that due to significantly fast operation of reserves, the myopic storage operation approaches the reliability improvements in the deterministic solutions, and hence can be used for real-time operation.

The rest of the paper is organized as follows. Section II introduces the reliability indices used and the formulations of the response aware storage operation to reduce imbalance. Section III provides optimization formulation for storage as reserve for different cost function. Section IV provides case studies for Elia in Belgium and BPA in the USA respectively. Section V concludes the paper.

2 RELIABILITY OF POWER GRIDS

The system average interruption duration index, SAIDI [1], is commonly used as a reliability indicator by electric power utilities.

SAIDI is the average outage duration for each customer served and is given as:

$$\text{SAIDI} = \frac{\text{Sum of customer interruption duration}}{\text{Total number of customers served}} = \frac{\sum U_i N_i}{C_T} \quad (1)$$

where N_i is the number of consumers for the outage time U_i for incident i . C_T is the total number of customers served. We define reliability index (RI) as

$$\text{RI} = \left(1 - \frac{\text{SAIDI in units of time}}{\text{Time horizon for calculating SAIDI}} \right) \quad (2)$$

Almost all developed countries have a power system reliability higher than 99.9%, that is expected to be ensured in the presence of renewables [1]. For research purposes, the detailed real-world information for faults and consumers affected by each fault needed for calculating SAIDI may be hard to get. Therefore, we redefine SAIDI in terms of the power imbalance in demand and supply relative to the aggregate load. We define residual $R(i) = \Delta_i + s_i$, where Δ_i and s_i denote net imbalance (without storage) and storage power output at time i , respectively. For our system, *modified* SAIDI is defined as

$$\text{SAIDI}^{\text{mod}} = \frac{\sum_i^{N_T} |R(i)|}{\bar{P}_g(i)} \quad (3)$$

where N_T is the total number of samples in the time horizon for SAIDI computation. \bar{P}_g is the mean of active power and is given as

$$\bar{P}_g = \frac{1}{N_T} \sum_{i=1}^{N_T} P_g(i). \quad (4)$$

Note that the sample based SAIDI definition, similar to the cost function in [29], intuitively assumes that the number of customers interrupted is captured in the size of power imbalance in the system. While our reliability measure increases with decreasing net imbalance, it does not account for the system response following an imbalance.

Including system response in reliability: In power grids, demand and supply are matched approximately at every time instant to maintain frequency within a narrow band as listed in Table 1. Ro-

Table 1: Continuous operating frequency range

Country	COFR
Germany[24], China [19]	49.5 to 50.5 Hz
Australia [19]	47 to 52 Hz
USA [24]	A-zone: 59.95 to 60.05 Hz, B-zone: 59.8-59.95 & 60.05-60.02 Hz, C-zone: <59.8 Hz & >60.02Hz

tational generators such as synchronous and induction machines in the grid provide an inherent rotational inertia as well as governor feedback (called Primary Frequency Control) that act to correct the operating frequency $f(t)$, following imbalance. This dynamics is modelled by the Swing equation [8, 22]:

$$\frac{df(t)}{dt} = \frac{1}{M_H} (P_m(t) - P_e(t)), \quad (5)$$

where P_m and P_e are the system's mechanical power and electrical load. M_H is the inertia in the system. Considering a system-wide ramp rate of C MW/s that provides frequency damping services,

the frequency nadir f_{\min} reached due to a net imbalance/residual $R(i)$ in the system is given by (see [8] for the derivation):

$$M_H C = \frac{R(i)}{2(f_0 - f_{\min} - f_{db})}. \quad (6)$$

Here f_0 is the normal operating frequency, while f_{db} is the dead-band frequency for governor response. This is derived in [8] by first determining the time to reach the frequency nadir from the event beginning and then using that to determine the system frequency. The operation of the primary response takes places within the first 30 seconds following an imbalance, as shown in Fig. 1. Note that a similar analysis can be conducted for frequency incursion above the rated frequency. If system inertia and ramp rates of different conventional generators are comparable (else consider the minimum per mW), then the total system inertia M_H and ramp rates C can each be considered proportional to the total scheduled generation P_g in the system. Going forward to regimes with similarly sized local generation (Eg. networked micro-grids), one can approximate $M_H C$ with a constant times P_g^2 , the square of the total system load. Consider a pre-fixed maximum frequency deviation $f_0 - f_{\min}$ for system safety. As dead-band f_{db} is pre-determined, it follows from Eq. (6) that the maximum imbalance $R(i)$ that the grid can safely sustain, is proportion to the scheduled system load or generation, as noted below.

$$-\epsilon P_g \leq R(i) = \Delta(i) + s_i \leq \epsilon P_g \quad (7)$$

Here ϵ is a constant that depends on system inertia and ramp rate. ϵ tends to 0 as the RES share tends towards 100% in the power network. Note that conservative operators can determine a lower ϵ to be on the safe side. To account for the system safety for small imbalances below ϵP_g , we modify the SAIDI^{mod} formula in Eq. (3) and define response-aware SAIDI _{ϵ} ^{mod} below.

$$\text{SAIDI}_{\epsilon}^{\text{mod}} = \frac{\sum_i \max(|R(i)| - \epsilon P_g(i), 0)}{\bar{P}_g(i)} \quad (8)$$

Using Eqs. (2,3,8) the reliability for our system, with and without response awareness, are respectively given by

$$\text{RI}^{\text{mod}} = \left(1 - \frac{1}{N_T} \frac{\sum_i |R(i)|}{\bar{P}_g(i)} \right) = \left(1 - \frac{\sum_i |R(i)|}{\sum_i P_g(i)} \right), \quad (9)$$

$$\text{RI}_{\epsilon}^{\text{mod}} = \left(1 - \frac{\sum_i \max(|R(i)| - \epsilon P_g(i), 0)}{\sum_i P_g(i)} \right). \quad (10)$$

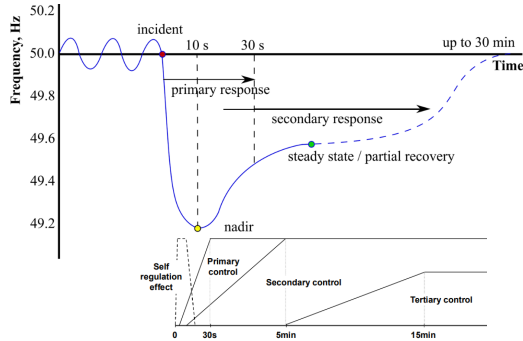


Figure 1: Reserves activation during a contingency [20]

Time-scale of battery operation: Note that we assume storage operation to be without delay after an imbalance is observed. In practice, such seamless storage operations can be conducted

through rate of change of frequency (RoCoF) measurements [12] directly or through the use of phasor measurement devices. In the next section, we describe the storage optimization problems that consider the defined reliability functions RI^{mod} and $\text{RI}_{\epsilon}^{\text{mod}}$ (with response awareness).

3 OPTIMIZATION OF STORAGE

In this section, we outline optimization formulations for battery performing supply-demand balancing considering (a) linear or quadratic cost function for minimizing imbalance, (b) response of the power network, (c) maintaining the SoC of the battery. While we first consider optimal deterministic solutions schemes over a time-horizon with perfect information of fluctuations, in real-world future information will not be available. Thus, we also provide myopic rule-based real-time algorithms and benchmark them against the optimal deterministic formulations. For normalized time-instance i , the battery energy b_i and power output s_i needs to satisfy the following constraints:

$$b_i \in [b_{\min}, b_{\max}], \quad s_i \in [S_{\min}, S_{\max}] \quad (11)$$

$$b_i = b_{i-1} + \max(s_i, 0)\eta_{ch} - \max(-s_i, 0)/\eta_{dis}. \quad (12)$$

where Eq.(11) reflects the bounds on b_i and s_i , and Eq.(12) describes the linear dynamics in b_i . η_{ch} and η_{dis} are the efficiencies of battery charging and discharging. State-of-charge of battery at time i is

$$\text{SoC}_i = b_i / b_{\text{rated}}, \quad (13)$$

where b_{rated} denotes the rated battery capacity.

3.1 Linear Cost Function

The linear cost function follow from the definition of RI^{mod} and $\text{RI}_{\epsilon}^{\text{mod}}$ in Eqs. (9) and (10) respectively. Under response awareness, the cost for imbalance below a threshold is 0. We first describe the case where system response is not considered in storage operation.

3.1.1 Reliability without response awareness. The optimization problem (P_L) is given as

$$(P_L) \min \sum_{i=1}^N |\Delta_i + s_i|, \quad \text{subject to (11, 12)}$$

Note that for a linear cost function, the non-zero net/marginal improvement made in reducing imbalance is the same irrespective of time-instant or overall imbalance magnitude. Thus, storage can be operated myopically considering only the current imbalance, using thresholds, as described in Algorithm 1.

Algorithm 1 Linear Cost without Response

Inputs: $\Delta = (\Delta_1, \Delta_2, \dots, \Delta_N)$, b_0 , **Parameters:**

$b_{\max}, b_{\min}, \delta_{\max}, \delta_{\min}, \eta_{ch}, \eta_{dis}$

Outputs: $s^* = (s_1^*, s_2^*, \dots, s_N^*)$, $b^* = (b_1^*, b_2^*, \dots, b_N^*)$

- 1: **if** $\Delta_i > 0$ **then** $s_i^* = \max\{-\Delta_i, \delta_{\min} h \eta_{dis}, (b_{\max} - b_{i-1}) \eta_{dis}\}$.
- 2: **else** $s_i^* = \min\{-\Delta_i, \delta_{\max} h / \eta_{ch}, (b_{\min} - b_{i-1}) / \eta_{ch}\}$.
- 3: **end if**
- 4: Update $b_i^* = b_{i-1}^* + \max(s_i^*, 0) \eta_{ch} - \max(-s_i^*, 0) / \eta_{dis}$.
- 5: Increment $i = i + 1$.

3.1.2 *Reliability with response awareness.* Based on RI_ϵ (see Eq. (10)), the optimization problem here is given by:

$$(P_L^\epsilon) \min \sum_{i=1}^N \{\max(|\Delta_i + s_i| - \epsilon P_g(i), 0)\}, \text{ subject to (11, 12)}$$

Problem (P_L^ϵ) can also be solved by a rule-based policy given in Algorithm 2 that differs from Algorithm 1 due to ϵ -induced thresholding in the cost-function.

Algorithm 2 Linear Cost with Response

Inputs: $\Delta = (\Delta_1, \dots, \Delta_N)$, b_0 , **Parameters:**

$b_{\max}, b_{\min}, \delta_{\max}, \delta_{\min}, \eta_{ch}, \eta_{dis}$

Outputs: $s^* = (s_1^*, s_2^*, \dots, s_N^*)$, $b^* = (b_1^*, b_2^*, \dots, b_N^*)$

- 1: **if** $\Delta_i > \epsilon P_g(i)$ **then**
 - 2: $s_i^* = \max\{-\Delta_i + \epsilon P_g(i), \delta_{\min} h \eta_{dis}, (b_{i-1} - b_{\max}) \eta_{dis}\}$,
 - 3: **else if** $\Delta_i \in (-\epsilon P_g(i), \epsilon P_g(i))$ **then** $s_i^* = 0$,
 - 4: **else** $s_i^* = \min\{-\Delta_i - \epsilon P_g(i), \delta_{\max} h / \eta_{ch}, b_{i-1} - b_{\min} / \eta_{ch}\}$.
 - 5: **end if**
 - 6: Update $b_i^* = b_{i-1}^* + \max(s_i^*, 0) \eta_{ch} - \max(-s_i^*, 0) / \eta_{dis}$.
 - 7: Increment $i = i + 1$.
-

3.2 Quadratic Cost Function

We now describe optimal storage actions where the cost for imbalance is quadratic. In this setting, imbalance minimization at larger imbalances are prioritize for storage operation.

3.2.1 *Reliability without response awareness.* The optimization problem for storage without response awareness is formulated as:

$$(P_Q) \min \sum_{i=1}^N (\Delta_i + s_i)^2, \quad \text{subject to (11, 12)}$$

Clearly, look-ahead is essential for solving (P_Q) , unlike (P_L) . However, standard convex optimization is sufficient to solve it as the cost function is smooth.

3.2.2 *Reliability with response awareness.* Under knowledge of system response, we use a quadratic cost that ignores imbalances below $\epsilon P_g(i)$, similar to the linear setting. The optimization problem is given by:

$$(P_Q^\epsilon) \min \sum_{i=1}^N \{\max(|\Delta_i + s_i| - \epsilon P_g(i), 0)\}^2, \text{ subject to (11, 12)}$$

The cost function in (P_Q^ϵ) is not smooth due to the absolute value operator. We use θ_i to denote $\max(|\Delta_i + s_i| - \epsilon P_g(i), 0)$, and then derive a McCormick relaxation [25] scheme for the absolute value operator to solve (P_Q^ϵ) , as described below.

$$(P_{Q1}^\epsilon) \min \sum_{i=1}^N \theta_i^2, \text{ subject to (a) (11), (b) (12),}$$

$$(c) \theta_i \geq 0, \quad \theta_i \geq 2z_i^1(\Delta_i + s_i) - (\Delta_i + s_i) - \epsilon P_g(i),$$

$$(d) \text{ McCormick Constraints for } y_i = z_i^1(\Delta_i + s_i)$$

$$y_i \geq \Delta_i^{lb} z_i, \quad y_i \geq (\Delta_i + s_i) + \Delta_i^{ub} z_i - \Delta_i^{ub}$$

$$y_i \leq \Delta_i^{ub} z_i, \quad y_i \leq (\Delta_i + s_i) + \Delta_i^{lb} z_i - \Delta_i^{lb}$$

$$(e) \text{ Binary variable: } 2y_i - (\Delta_i + s_i) \geq 0.$$

where $\Delta_i^{lb} = \Delta_i + S_{\min}$, $\Delta_i^{ub} = \Delta_i + S_{\max}$, z_i denotes a binary variable which is equal to 1 when net imbalance with storage, $(\Delta_i + s_i)$ is positive. Note that the McCormick relaxation is used to approximate the values of a bilinear variable by creating a quadrilateral feasible space bounded by 4 constraints derived using the upper and lower limits of the individual variables in the bilinear variable. This form is exact when one of the variables in the bilinear form is binary [25]. Here $y_i = z_i(\Delta_i + s_i)$ has a binary component z_i .

Note that the storage SoC is not included in the optimization problems discussed till now. An operator may be interested in keeping SoC within a certain band to ensure available storage for future unforecasted large fluctuations. Next we discuss formulations where SoC targets are promoted through penalized SoC deviations.

3.3 Reliability with response awareness and SoC management

Consider the setting where storage SoC needs to be maintained within a band, denoted as $[\text{SoC}_l, \text{SoC}_u]$, where $\text{SoC}_l, \text{SoC}_u$ denote the lower and upper boundaries, and mean SoC level is denoted as $\text{SoC} = 0.5 \times (\text{SoC}_l + \text{SoC}_u)$. We define γ as $\gamma = \text{SoC} - \text{SoC}_l = \text{SoC}_u - \text{SoC}$. Denote $\theta_i = \max(|\Delta_i + s_i| - \epsilon P_g(i), 0)$ and $\beta_i = \lambda \max(|\text{SoC}_i - \text{SoC}| - \gamma, 0)$. The objective of storage optimization under response awareness and SoC management for linear cost for imbalance is given as

$$(P_{LS}^\epsilon) \min \sum_{i=1}^N \{\theta_i + \beta_i\}, \quad \text{subject to (11, 12, 13).}$$

On the other hand, the objective with quadratic cost for imbalance is given as

$$(P_{QS}^\epsilon) \min \sum_{i=1}^N \{\theta_i + \beta_i\}^2, \quad \text{subject to (11, 12, 13).}$$

Note that with SoC management, the optimal solutions for both linear and quadratic cost formulations do not have an optimal myopic form. We, thus, revert to two McCormick relaxation schemes to overcome the non-smooth parts of the cost function (one for reliability, another for SoC). The additional associated constraints for both P_{LS}^ϵ and P_{QS}^ϵ are given by:

$$(c) \theta_i \geq 0, \quad \theta_i \geq 2z_i^1(\Delta_i + s_i) - (\Delta_i + s_i) - \epsilon P_g(i),$$

$$(d) \beta_i \geq 0, \quad \beta_i \geq 2z_i^2 \text{SoC}_i - 2z_i^2 \text{SoC} - \text{SoC}_i + \text{SoC} - \gamma,$$

$$(e) \text{ McCormick Constraints for } y_i^1 = z_i^1(\Delta_i + s_i)$$

$$y_i^1 \geq \Delta_i^{lb} z_i^1, \quad y_i^1 \geq (\Delta_i + s_i) + \Delta_i^{ub} z_i^1 - \Delta_i^{ub}$$

$$y_i^1 \leq \Delta_i^{ub} z_i^1, \quad y_i^1 \leq (\Delta_i + s_i) + \Delta_i^{lb} z_i^1 - \Delta_i^{lb}$$

$$(e) \text{ McCormick Constraints for } y_i^2 = z_i^2 \text{SoC}_i$$

$$y_i^2 \geq \text{SoC}_{\min} z_i^2, \quad y_i^2 \geq \text{SoC}_i + \text{SoC}_{\max} z_i^2 - \text{SoC}_{\max}$$

$$y_i^2 \leq \text{SoC}_{\max} z_i^2, \quad y_i^2 \leq \text{SoC}_i + \text{SoC}_{\min} z_i^2 - \text{SoC}_{\min}$$

$$(e) \text{ Binary variable: } 2y_i^1 - (\Delta_i + s_i) \geq 0,$$

$$2y_i^2 - \text{SoC}_i \geq 0.$$

where $\Delta_i^{lb} = \Delta_i + S_{\min}$, $\Delta_i^{ub} = \Delta_i + S_{\max}$, z_i^1 denotes a binary variable which is equal to 1 when $(\Delta_i + s_i)$ is positive. z_i^2 denotes another binary variable which is equal to 1 when $\text{SoC}_i - \text{SoC} \geq 0$ is positive.

3.4 Myopic control considering SoC & inertia

Storage control in the real-world will not have access to accurate information of future imbalances. In those settings, optimal solutions for problems (P_{LS}^ϵ) and (P_{QS}^ϵ) that require perfect information will not be practical. Instead, we propose a myopic Algorithm 3 in this section, for linear cost on reliability with response awareness and SoC management. Algorithm 3 is thus an extension of Algorithm 2. It uses the current information (SoC and imbalance in the power network) and network response to make charge/discharge decisions to minimize the imbalance. When the imbalance is within bounds (see Eq. (7)), it also attempts to keep the SoC within the desired SoC band. Lines 3 to 6 decides whether the SoC is outside the target band. The SoC target band is decided based on battery type. For example, Lilon battery cannot be over-charged above an SoC level or over-discharged below a certain level [13]. Similarly, the zones for imbalance is identified in Algorithm 3's lines 7 to 11. The storage operation is further constrained by capacity and ramping constraint. Based on the SoC and imbalance levels designated by Flag_{SoC} and Flag_Δ respectively, different combinations are possible. The respective actions under each case are described in lines 12-34 of the pseudo code. The algorithm can be similarly extended to derive a sub-optimal myopic policy for quadratic costs. In the next section, we provide simulation results on benefits from storage usage in reliability using real power grid imbalance data.

4 NUMERICAL SIMULATIONS

To compare benefits from our optimization algorithms for different cost functions and constraints, we use following performance indices: (a) Linear deviation: (λ_{linear}) equals $\sum_{i=1}^N \{\max(|\Delta_i + s_i| - \epsilon P_g(i), 0)\} \times 100 / \bar{P}_g(i)$, (b) Quadratic deviation: (λ_{quad}) equals $\sum_{i=1}^N \{\max(|\Delta_i + s_i| - \epsilon P_g(i), 0)\}^2 \times 100 / (\bar{P}_g(i))^2$, (c) SAID $_\epsilon^{\text{mod}}$ and Reliability index $\text{RI}_\epsilon^{\text{mod}}$, and (d) Mean SoC.

4.1 Imbalance minimization in Elia, Belgium

The data considered in this case study is from the month of January 2019. Fig. 2 shows the aggregate load, demand and supply imbalance and the imbalance in percentage with respect to the aggregate load. Without storage, the reliability RI^{mod} is equal to 98.845%. SAID $^{\text{mod}}$ for this month is 515.5 minutes. Observe that at hour index 253, an imbalance of the order of 17% with respect to the total load occurs, due to a sudden loss of generation of approximately 2000 MW. The reserve sizing necessary to completely mitigate this unbalance will require an astounding ramping capability of 2000 MW or more.

The objective of study for the Elia data is to identify the marginal value of adding storage as reserves, for different values of system response, that is measured in terms of ϵ (see Eq. (7,8)). We vary ϵ from 0 to 5% and implement the following 5 storage settings:

(i) No storage (nominal case), (ii) with 100 MW 1C-1C¹, (iii) with 200 MW 1C-1C, (iv) with 500 MW 1C-1C, (v) with 1000 MW 1C-1C.

Fig. 3 belabors the fact that the benefit of storage sizing for reliability is higher at lower ϵ (less conventional reserves), which is the regime of operation for grids with high renewable penetration.

¹Battery model xC-yC means that the battery takes 1/x hours to charge from completely discharged state at the maximum charging rate and 1/y hours to discharge from completely charged state at the maximum discharging rate

Algorithm 3 Myopic Algorithm with Linear Cost with Response, and SoC consideration

Inputs: $\Delta = (\Delta_1, \Delta_2, \dots, \Delta_N)$, b_0 , **Parameters:** $b_{\text{max}}, b_{\text{min}}, \delta_{\text{max}}, \delta_{\text{min}}, \eta_{\text{ch}}, \eta_{\text{dis}}$, **Initialize:** $\text{SoC}_u, \text{SoC}_l, b_{\text{rated}}$
Outputs: $s^* = (s_1^*, s_2^*, \dots, s_N^*)$, $b^* = (b_1^*, b_2^*, \dots, b_N^*)$

- 1: Calculate $\text{SoC}_i = b_i / b_{\text{rated}}$ and $\text{SoC} = 0.5 \times (\text{SoC}_l + \text{SoC}_u)$
- 2: **if** $\text{SoC}_i \leq \text{SoC}_l$ **then** $\text{Flag}_{\text{SoC}} = 1$,
- 3: **else if** $\text{SoC}_i > \text{SoC}_l$ and $\text{SoC}_i \leq \text{SoC}_u$ **then** $\text{Flag}_{\text{SoC}} = 2$,
- 4: **else** $\text{Flag}_{\text{SoC}} = 3$,
- 5: **end if**
- 6: $\Delta_{\text{min}} = -\epsilon P_g(i)$, $\Delta_{\text{max}} = \epsilon P_g(i)$
- 7: **if** $\Delta_i \leq \Delta_{\text{min}}$ **then** $\text{Flag}_\Delta = 1$,
- 8: **else if** $\Delta_i > \Delta_{\text{min}}$ and $\Delta_i \leq \Delta_{\text{max}}$ **then** $\text{Flag}_\Delta = 2$,
- 9: **else** $\text{Flag}_\Delta = 3$,
- 10: **end if**
- 11: **if** $\text{Flag}_{\text{SoC}} == 1$ and $\text{Flag}_\Delta == 1$ **then** Charge, $s_i^* =$
- 12: $\max\{\min\{\delta_{\text{max}} h / \eta_{\text{ch}}, (\text{SoC}_u - \text{SoC}_i) b_{\text{rated}} / \eta_{\text{ch}}, -\Delta_i - \epsilon P_g(i)\}, 0\}$,
- 13: **else if** $\text{Flag}_{\text{SoC}} == 1$ and $\text{Flag}_\Delta == 2$ **then** Replenish charge, $s_i^* =$
- 14: $\max\{\min\{\delta_{\text{max}} h / \eta_{\text{ch}}, (\text{SoC} - \text{SoC}_i) b_{\text{rated}} / \eta_{\text{ch}}, -\Delta_i + \epsilon P_g(i)\}, 0\}$,
- 15: **else if** $\text{Flag}_{\text{SoC}} == 1$ and $\text{Flag}_\Delta == 3$ **then**
- 16: Do nothing, $s_i^* = 0$,
- 17: **else if** $\text{Flag}_{\text{SoC}} == 2$ and $\text{Flag}_\Delta == 1$ **then** Charge, $s_i^* =$
- 18: $\max\{\min\{\delta_{\text{max}} h / \eta_{\text{ch}}, (\text{SoC}_u - \text{SoC}_i) b_{\text{rated}} / \eta_{\text{ch}}, -\Delta_i - \epsilon P_g(i)\}, 0\}$,
- 19: **else if** $\text{Flag}_{\text{SoC}} == 2$ and $\text{Flag}_\Delta == 2$ **then**
- 20: **if** $\text{SoC}_i \leq \text{SoC}$ **then** Replenish charge, $s_i^* =$
- 21: $\max\{\min\{\delta_{\text{max}} h / \eta_{\text{ch}}, (\text{SoC} - \text{SoC}_i) b_{\text{rated}} / \eta_{\text{ch}}, -\Delta_i + \epsilon P_g(i)\}, 0\}$,
- 22: **else** Replenish charge, $s_i^* =$
- 23: $\min\{\max\{\delta_{\text{min}} h \eta_{\text{dis}}, (\text{SoC} - \text{SoC}_i) b_{\text{rated}} \eta_{\text{dis}}, -\Delta_i - \epsilon P_g(i)\}, 0\}$,
- 24: **end if**
- 25: **else if** $\text{Flag}_{\text{SoC}} == 2$ and $\text{Flag}_\Delta == 3$ **then** Discharge, $s_i^* =$
- 26: $\min\{\max\{\delta_{\text{min}} h \eta_{\text{dis}}, (\text{SoC}_l - \text{SoC}_i) b_{\text{rated}} \eta_{\text{dis}}, -\Delta_i - \epsilon P_g(i)\}, 0\}$,
- 27: **else if** $\text{Flag}_{\text{SoC}} == 3$ and $\text{Flag}_\Delta == 1$ **then**
- 28: Do nothing, $s_i^* = 0$,
- 29: **else if** $\text{Flag}_{\text{SoC}} == 3$ and $\text{Flag}_\Delta == 2$ **then** Replenish charge, $s_i^* =$
- 30: $\min\{\max\{\delta_{\text{min}} h \eta_{\text{dis}}, (\text{SoC} - \text{SoC}_i) b_{\text{rated}} \eta_{\text{dis}}, -\Delta_i - \epsilon P_g(i)\}, 0\}$,
- 31: **else if** $\text{Flag}_{\text{SoC}} == 3$ and $\text{Flag}_\Delta == 3$ **then** Discharge, $s_i^* =$
- 32: $\min\{\max\{\delta_{\text{min}} h \eta_{\text{dis}}, (\text{SoC}_l - \text{SoC}_i) b_{\text{rated}} \eta_{\text{dis}}, -\Delta_i - \epsilon P_g(i)\}, 0\}$,
- 33: **end if**
- 34: Update $b_i^* = b_{i-1}^* + [s_i^*]^+ \eta_{\text{ch}} - [s_i^*]^- / \eta_{\text{dis}}$ and Increment $i = i + 1$.

From Fig. 4, it is clear that the marginal benefit in reliability due to storage decreases with increasing storage sizes, as expected. However, note that the decay in marginal benefit due to increasing storage is much sharper at higher system response ϵ . This suggests that analysis on greater installation of storage in a grid should involve thorough studies of current and future trends in conventional reserve availability. The myopic control Algorithm 3 is used for the optimization with linear cost, but takes into account system response ($\epsilon = .5\%$) and SoC maintenance within 40% – 80% band. Whenever the SoC dips below the minimum level or rises above the maximum, the controller follows by re-adjusting the SoC, during time instants when the imbalance R_i is within the response-aware bound in Eq. (7).

4.2 Imbalance minimization in BPA, USA

We now consider the aggregated load and generation variation in BPA, for 6 days starting from May 10 2019, collected from their website [2]. Using this data, we compare the performance of our

optimization schemes for linear and quadratic cost functions (with differing system responses), for a 1C-1C battery of capacity 100 MW. The results are provided in Table. 2. Observe that the reliability RI_{ϵ}^{mod} for the myopic scheme with linear costs with response awareness and SoC, approaches that of the deterministic scheme that uses full information of all fluctuations. Note that the RI_{ϵ}^{mod} for no storage case for $\epsilon = 0.05$ is 99.9197 %. For deterministic linear cost function $RI_{\epsilon}^{mod} = 99.965$ %, for quadratic cost function $RI_{\epsilon}^{mod} = 99.966$ %. For cost functions also considering SoC regulation constraint the reliability improvement for linear and quadratic deteriorates to 99.923. All the above results are for deterministic (complete information) setting. In comparison, the myopic algorithm with no look-ahead provides a reliability level of 99.943.

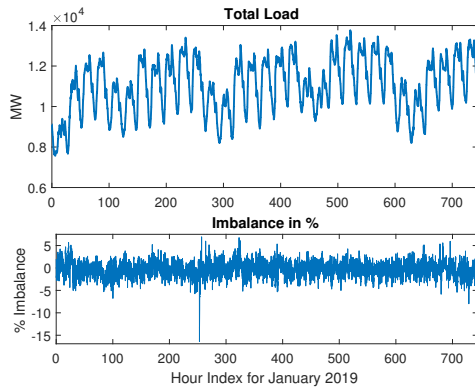


Figure 2: Load and percentage of imbalance in Elia on January 2019. Loss of a generation (≈ 2000 MW) on 10th January 2019 around 13:00h; the load curve is not affected as the generation loss happens.

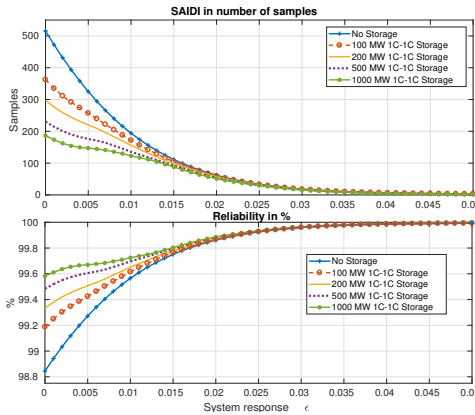


Figure 3: Reliability (RI_{ϵ}^{mod}) and $SAIDI_{\epsilon}^{mod}$ calculated with varying system response (ϵ) and storage size in Elia.

Although, slightly lower than linear and quadratic cost functions, it is superior compared to deterministic setting with SoC regulation. The myopic algorithm performs significantly well primarily because of the fast sampling time. A similar observation is made in [7] where myopic stochastic control has an optimality gap of less than 4% compared to the ground truth.

5 CONCLUSION AND PERSPECTIVES

The paper presents algorithms for control of energy storage for minimizing macroscopic demand and supply imbalance. Through

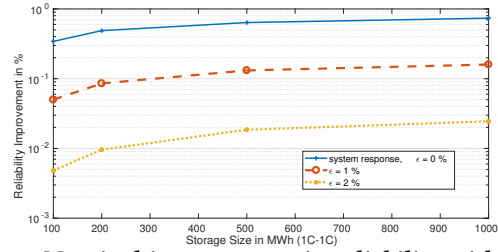


Figure 4: Marginal improvement in reliability with energy storage in Elia.

Table 2: Performance Indices for BPA for period 10 to 15 May 2019; 1C-1C battery of capacity 100 MW.

Optimization ϵ	λ_{linear}	λ_{quad}	SoS	$SAIDI_{\epsilon}^{mod}$	RI_{ϵ}^{mod}	
No storage	0	3245.7	114.5	-	32.45	98.1228
	0.001	3077.1	108.1	-	30.77	98.2203
	0.005	2480.7	85.6	-	24.81	98.5652
	0.01	1893.8	63.5	-	18.94	98.9047
Linear + response	0	1295.1	48.1	0.6567	23.18	98.6592
	0.001	2168.2	85.2	0.4060	21.68	98.7460
	0.005	1656.1	62.2	0.3958	16.562	99.0421
Quadratic with response	0	1183.9	41.4	0.3939	11.839	99.3153
	0.001	1171.0	32.9	0.5222	23.23	98.6564
	0.001	2165.0	62.9	0.5146	21.60	98.7505
Linear + response + SoC	0.005	1656.0	47.5	0.5096	16.52	99.0447
	0.01	1188.6	33.1	0.4963	12.03	99.3044
	0.001	2175.4	81.8	0.6220	29.95	98.2681
Quadratic + SoC + response	0.005	1689.6	61.6	0.6496	24.01	98.6110
	0.01	1214.0	42.7	0.6722	16.02	99.0732
	0.001	2168.7	62.9	0.5210	22.28	98.7112
Myopic with linear + Response + SoC	0.005	1685.6	47.6	0.5590	19.62	98.8649
	0.01	1211.9	33.1	0.6063	15.98	99.0756
	0	1436.7	50.6	0.6377	23.18	98.6592
with linear + Response + SoC	0.001	1437.2	50.6	0.6394	22.80	98.6811
	0.005	1440.8	51.4	0.6164	20.35	98.8228
	0.01	1417.5	51.7	0.6278	15.818	99.0851

theoretical motivation corroborated with numerical simulations, we show that the system dynamic response due to inertia and governor control, impacts the effect of storage in improving grid reliability. In particular, the marginal reliability benefit due to increasing storage decays rapidly for systems with higher conventional reserves. For real-time optimization of storage, we present myopic alternates to deterministic storage algorithms requiring full information, and show their comparable performance using real data from Elia, Belgium and BPA, USA. Furthermore, we demonstrate that storage control algorithms can maintain SoC without significant loss in reliability performance.

In future work, we plan to theoretically study the relationship between variance of stochastic imbalances, and response aware storage operation. Moreover, we plan to extend our numerical analysis to smaller grids/micro-grids with greater fraction of inverter-connected generation, and study financial incentives to maximize reliability performance from storage.

REFERENCES

- [1] 2013. Forging a Path toward a Digital Grid Global perspectives on smart grid opportunities. Accenture's Digitally Enabled Grid program, <https://tinyurl.com/yymtdod>. (2013).
- [2] 2019. BPA Balancing Reserves Deployed. Imbalance signal BPA, <https://transmission.bpa.gov/business/operations/Wind/reserves.aspx>. (2019).
- [3] 2019. A Behind the Scenes Take on Lithium-ion Battery Prices. BloombergNEF article, <https://about.bnef.com/blog/behind-scenes-take-lithium-ion-battery-price>. (2019).
- [4] 2019. Managing oversupply: Oversupply and curtailments. CAISO cutrilmnt report, <http://www.caiso.com/informed/Pages/ManagingOversupply.aspx>. (2019).
- [5] Hossein Akhavan-Hejazi and Hamed Mohsenian-Rad. 2013. Optimal operation of independent storage systems in energy and reserve markets with high wind penetration. *IEEE Transactions on Smart Grid* 5, 2 (2013), 1088–1097.
- [6] Kyle Bradbury, Lincoln Pratson, and Dalia Patiño-Echeverri. 2014. Economic viability of energy storage systems based on price arbitrage potential in real-time US electricity markets. *Applied Energy* 114 (2014), 512–519.
- [7] Ana Bušić, Md Umar Hashmi, and Sean Meyn. 2017. Distributed control of a fleet of batteries. In *2017 American Control Conference (ACC)*. IEEE, 3406–3411.
- [8] Héctor Chávez, Ross Baldick, and Sandip Sharma. 2014. Governor rate-constrained OPF for primary frequency control adequacy. *IEEE Transactions on Power Systems* 29, 3 (2014), 1473–1480.
- [9] George Crabtree, Jim Misewich, Ron Ambrosio, Kathryn Clay, Paul DeMartini, Revis James, Mark Lauby, Vivek Mohta, John Moura, Peter Sauer, et al. 2011. Integrating renewable electricity on the grid. In *AIP Conference proceedings*, Vol. 1401. AIP, 387–405.
- [10] Kaushik Das, Marisciel Litong-Palima, Petr Maule, and Poul E Sørensen. 2015. Adequacy of operating reserves for power systems in future european wind power scenarios. In *2015 IEEE Power & Energy Society General Meeting*. IEEE, 1–5.
- [11] Gauthier Delille, Bruno Francois, and Gilles Malarange. 2012. Dynamic frequency control support by energy storage to reduce the impact of wind and solar generation on isolated power system's inertia. *IEEE Transactions on Sustainable Energy* 3, 4 (2012), 931–939.
- [12] DM Greenwood, Khim Yan Lim, C Patsios, PF Lyons, Yun Seng Lim, and PC Taylor. 2017. Frequency response services designed for energy storage. *Applied Energy* 203 (2017), 115–127.
- [13] Md Umar Hashmi. 2019. *Optimization and control of storage in smart grids*. Ph.D. Dissertation. PSL Research University.
- [14] Md Umar Hashmi, Deepjyoti Deka, Ana Busic, Lucas Pereira, and Scott Backhaus. 2020. Arbitrage with power factor correction using energy storage. *IEEE Transactions on Power Systems* (2020).
- [15] Md Umar Hashmi, Deepan Muthirayan, and Ana Bušić. 2018. Effect of Real-Time Electricity Pricing on Ancillary Service Requirements. In *Proceedings of the Ninth International Conference on Future Energy Systems*. ACM, 550–555.
- [16] Md Umar Hashmi, Lucas Pereira, and Ana Busic. 2019. Energy Storage Roles in Madeira, Portugal: Co-Optimizing for Arbitrage, Self-Sufficiency, Peak Shaving and Energy Backup. In *IEEE PES Powertech, Milan*.
- [17] Cody A Hill, Matthew Clayton Such, Dongmei Chen, Juan Gonzalez, and W Mack Grady. 2012. Battery energy storage for enabling integration of distributed solar power generation. *IEEE Transactions on smart grid* 3, 2 (2012), 850–857.
- [18] Hannele Holttinen. 2008. Estimating the impacts of wind power on power systems—summary of IEA Wind collaboration. *Environmental research letters* 3, 2 (2008), 025001.
- [19] Jahangir Hossain and Apel Mahmud. 2014. *Large scale renewable power generation: advances in technologies for generation, transmission and storage*. Springer Science & Business Media.
- [20] Sebastian Just. 2015. The german market for system reserve capacity and balancing. (2015).
- [21] Vaclav Knap, Sanjay K Chaudhary, Daniel-Ioan Stroe, Maciej Swierczynski, Bogdan-Ionut Craciun, and Remus Teodorescu. 2015. Sizing of an energy storage system for grid inertial response and primary frequency reserve. *IEEE Transactions on Power Systems* 31, 5 (2015), 3447–3456.
- [22] Prabha Kundur. [n. d.]. *Power system stability and control*. Vol. 7.
- [23] Jason Leadbetter and Lukas Swan. 2012. Battery storage system for residential electricity peak demand shaving. *Energy and buildings* 55 (2012), 685–692.
- [24] Ivan Machado and Itzel Arias. 2006. Grid Codes Comparison. (2006).
- [25] Garth P McCormick. 1976. Computability of global solutions to factorable non-convex programs: Part I—Convex underestimating problems. *Mathematical programming* 10, 1 (1976), 147–175.
- [26] Amir-Hamed Mohsenian-Rad and Alberto Leon-Garcia. 2010. Optimal residential load control with price prediction in real-time electricity pricing environments. *IEEE Trans. Smart Grid* 1, 2 (2010), 120–133.
- [27] Alexandre Oudalov, Daniel Chartouni, and Christian Ohler. 2007. Optimizing a battery energy storage system for primary frequency control. *IEEE Transactions on Power Systems* 22, 3 (2007), 1259–1266.
- [28] Alexandre Oudalov, Rachid Cherkaoui, and Antoine Beguin. 2007. Sizing and optimal operation of battery energy storage system for peak shaving application. In *Power Tech, 2007 IEEE Lausanne*. IEEE, 621–625.
- [29] Han-I Su and Abbas El Gamal. 2013. Modeling and analysis of the role of energy storage for renewable integration: Power balancing. *IEEE Transactions on Power Systems* 28, 4 (2013), 4109–4117.
- [30] Stefan Weitemeyer, David Kleinhans, Thomas Vogt, and Carsten Agert. 2015. Integration of Renewable Energy Sources in future power systems: The role of storage. *Renewable Energy* 75 (2015), 14–20.
- [31] Peng Zou, Qixin Chen, Qing Xia, Guannan He, and Chongqing Kang. 2015. Evaluating the contribution of energy storages to support large-scale renewable generation in joint energy and ancillary service markets. *IEEE Transactions on Sustainable Energy* 7, 2 (2015), 808–818.